Jia LI, Xiao-Bing ZHANG, Naman RECHO*

Criterion Study of an Elastic-Plastic Tensile Crack by Using the Full Solution of the Stress Field

* Research Laboratory in Structural Mechanics (LERMES), Blaise Pascal University of Clermont-Ferrand, Av. Aristide Briand, 03100 Montluçon, France

Keywords: Asymptotic Behaviour, Elastic-plastic fracture mechanics, Cleavage fracture, Slip fracture, Failure criteria

ABSTRACT: *No satisfactory analytical solution of full elastic-plastic stress field has been found so far for plane strain mode I crack. Only the finite-element analyses have been developed on this topic. Recently, we proposed an energy variational method to study the full elastic-plastic field of the mode I crack under small-scale yielding conditions. Algebraic expression of the full stress field can be obtained to connect the near-tip plastic field to the far elastic one.Full stress fields have been obtained surrounding the crack tip for several types of specimens. The comparison with the results obtained by the fine finite-element analysis shows that this method is highly accurate in the whole region considered, whether for the near-tip field or for the far field. The algebraic expression of the stress fields allows us to examine these fields in detail. The trajectory lines of the principal stresses (the cleavage lines) and those of maximum shear stresses (the slip lines) of several specimens have been drown. In mode I plane strain, the maximum tensile stress is always along the crack plane, all cleavage lines near the crack tip go toward this direction and form a cleavage band. This means that the crack will progress in its own plane if the growth is created by cleavage. However, the maximum shear stresses are oriented at diverse angles with respect to the crack plane according to the geometry and loading of the specimen. It is found that the slip lines go always toward a few directions from the crack tip and form some slip line bands. The slip bands indicate clearly the direction of the plastic flaw, i.e. the direction of crack growth by slipping. The crack propagation depends on the competition between the maximum tensile stress at a critical distance $\sigma_{\theta\theta}(r_{IC})$ along the cleavage band and the shear stress at a critical distance $\tau(r_{IIC})$ along the slip band. Going from the expression of the full stress field this paper proposes a numerical method allowing to determine the type of crack growth in elastic plastic medium.*

Introduction

In elastic plastic medium the stress field near the crack tip can be determined by local asymptotic analysis, such as HRR solution [1],[2]. This stress field seems to be non-consistent when the strain field is large. This can be corrected by the use of a full analysis including the far field. In large strain elastic plastic medium the failure presents a computational aspect between two failure mechanisms.

The first one, cleavage failure, is due to circonferential opening stresses $\sigma_{\theta\theta}$ (named σ in the paper) or to the energy release rate G (which can be presented as a J-integral) when $\sigma_{\theta\theta}$, G, or J reach critical values σ_c (at certain distance r_c from the crack tip), G_c or J_c , the failure occurs.

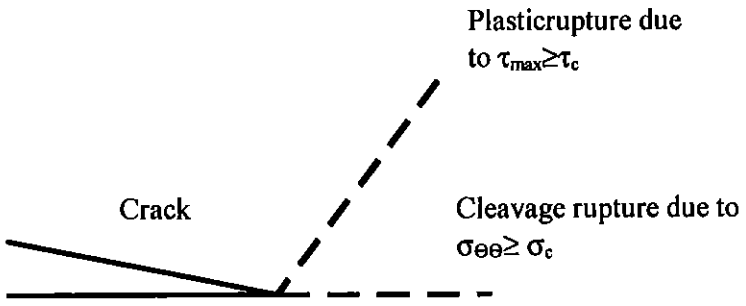

The second failure mechanism, slip failure, is due to very high local strains involving failure following a slip band in the direction of the maximum shear stress τ. The failure mechanism occurs when τ reaches τ_c the critical value of τ.

In order to show the influence of each failure mechanism we study an edge crack plate specimen under tensile load, in which the ratio of the crack length (a) to the plate width (w) varies such as $\frac{a}{w} = 0{,}1$; 0,5 or 0,9. When $\frac{a}{w}$ is growing τ is decreasing, in the same time $\sigma_{\theta\theta}$ is increasing. The fracture criteria $\tau > \tau_c$ or $\sigma_{\theta\theta} > \sigma_c$ will manage then the type of failure mechanism.

Going from a finite element analysis for each $\frac{a}{w}$ ratio. Such as analysis allows us to determine boundary conditions near the crack tip. These boundary conditions are used then in our analysis in order to provide full elastic-plastic solution which relates the local stress field (inner field) to the far stress field (outer field).

The aims of the paper are twofold :

First is to give more accurate elastic-plastic solution near the crack tip.

Second is to give the basis of failure criteria (slip failure, cleavage failure) and to determine the static conditions of the studied structure which privilege one of the two mechanisms of failure.

Computation Procedure

Description of the method

The energy variational method proposed by LI [3] is adapted in this work to study the full elastic-plastic stress field of a mode I crack. The main idea of this method is to establish a statically admissible stress field around the crack tip (inner field) connected continuously to the far stress field (outer field). The unknown parameters can be adjusted by minimizing the complementary energy of the structure.

Consider a material which deforms according to the Ramberg-Osgood stress-strain relationship, namely:

$$\varepsilon_{ij} = \frac{1+\nu}{E} s_{ij} + \frac{1-2\nu}{3E}\sigma_{kk}\delta_{ij} + \frac{3\alpha}{2E}\left(\frac{\sigma_e}{\sigma_0}\right)^{n-1} s_{ij} \tag{1}$$

where ε_{ij} are the strain components, s_{ij} the deviatoric stress components, σ_{kk} is the hydrostatic stress, E the elastic modulus, ν Poisson's ratio, δ_{ij} the Kronecker delta, α a material constant, n the hardening exponent, σ_0 the yielding stress, and σ_e the Mises equivalent effective stress defined as follows:

$$\sigma_e = (3/2\, s_{ij}\, s_{ij})^{1/2} \tag{2}$$

The inner stress field around the crack tip is assumed to be derived from a four-term expansion of the stress function ϕ_{in}:

$$\phi_{in} = r^{s0}\tilde{\phi}_0(\theta) + r^{s1}\tilde{\phi}_1(\theta) + r^{s2}\tilde{\phi}_2(\theta) + r^{s3}\tilde{\phi}_3(\theta) \tag{3}$$

where r and θ are the polar coordinates whose origin is the crack-tip; $\tilde{\phi}_0(\theta), \tilde{\phi}_1(\theta)$ ... are angular dependent functions and s_0, s_1, ... undetermined exponents with $s_0 < s_1 < \ldots$. The first term of (3) is the asymptotic field of the HRR solution. The last three terms can be determined by the variational technique.

For more convenience, we suppose that $\tilde{\phi}_0(\theta), \tilde{\phi}_1(\theta)$, ... can be approached by using a series of basic functions, such as polynomial functions of order q:

$$\phi_i(\theta) = \sum_{j=0}^{q} a_{ij}\theta^j \tag{4}$$

The coefficients a_{0j} can be calculated by developing the HRR solution into polynomial functions, while the coefficients a_{ij} (i>0) can be determined by considering the continuity between the inner and outer fields.

Suppose that the outer field is already known by its stress function ϕ_{out}. Similarly to (4), ϕ_{out} and its partial direvatives with respect to r at a circle boundary $r=R$ can also be developed into the polynomial functions of order q:

$$\begin{aligned}
\phi_{out}(r=R) &= \sum_{j=0}^{q} b_{0j}\theta^{j} \\
\frac{\partial \phi_{out}(r=R)}{\partial r} &= \sum_{j=0}^{q} b_{1j}\theta^{j} \\
\frac{\partial^2 \phi_{out}(r=R)}{\partial r^2} &= \sum_{j=0}^{q} b_{2j}\theta^{j}
\end{aligned} \tag{5}$$

The inner field and the outer field must be connected continuously across the circle boundary $r=R$. This condition leads to the following equation:

$$[\mathbf{A}] = [\mathbf{R}]^{-1}[\mathbf{B}] \tag{6}$$

where **[A]** is the unknown constant matrix and $[\mathbf{A}]=[a_{ij}]$, i=1,2,3; j=0,1,...q;

[R] is a constant matrix of dimension 3×3 and:

$$[\mathbf{R}] = \begin{bmatrix} R^{s1} & R^{s2} & R^{s3} \\ s_1 R^{s1-1} & s_2 R^{s2-1} & s_3 R^{s3-1} \\ s_1(s_1-1)R^{s1-2} & s_2(s_2-1)R^{s2-2} & s_3(s_3-1)R^{s3-2} \end{bmatrix} \tag{7}$$

[B] is a constant matrix of dimension 3×(q+1) and:

$$[\mathbf{B}] = \begin{bmatrix} b_{00} - R^{s0}a_{00} & b_{01} - R^{s0}a_{01} & \cdots \\ b_{10} - s_0 R^{s0-1}a_{00} & b_{11} - s_0 R^{s0-1}a_{01} & \cdots \\ b_{20} - s_0(s_0-1)R^{s0-2}a_{00} & b_{21} - s_0(s_0-1)R^{s0-2}a_{01} & \cdots \end{bmatrix} \tag{8}$$

From (6)~(8), all unknown constants a_{ij} can be obtained by a simple matrix multiplication. To determine the 3 exponents s_1, s_2 and s_3, the theorem of the minimum complementary energy is used. The complementary energy U_c of a structure in which the material follows

the stress-strain relationship defined by (1) for either plane stress or plane strain is:

$$U_c = \int_{\Omega}\left[\frac{1+\nu}{3E}\sigma_e^{\,2} + \frac{1-2\nu}{6E}\sigma_{kk}^{\,2} + \frac{\alpha\sigma_0^{\,2}}{E(n+1)}\left(\frac{\sigma_e}{\sigma_0}\right)^{n+1}\right]d\Omega \qquad (9)$$

The integration is calculated in the circle area $\Omega\in\ r<R$. The variation of the statically admissible stress can be completed by varying the exponents s_i. The problem then consists in finding out the parameters (s_1, s_2 ,s_3) so that the complementary energy becomes stationary and minimum. This minimization problem can be solved by using numerical methods.

By substituting (s_1, s_2 ,s_3) into (6), all coefficients a_{ij} can be determined. The stress function of the inner field is completely defined by (3).

Numerical procedures

The plane-strain crack-tip stress field is determined by using the energy method associated with the finite element modelling. The far stress field at the circle boundary $r=R$ is given by the FEM which does not need to be very fine. The FEM results allows us to verify the accuracy of the energy variational method in the elastic-plastic zone near the crack tip.

In general, the finite-element analysis only gives the stress components at the circle boundary. From these stress components, the stress function and its derivatives with respect to r can be calculated by following equations:

$$\begin{aligned}
&\phi_{out}(R,\theta) = R^2\left\{\sin\theta\int_{\pi}^{\theta} f(\theta)\cos\theta d\theta - \cos\theta\int_{\pi}^{\theta} f(\theta)\sin\theta d\theta\right\}\\
&\frac{\partial\phi_{out}(R,\theta)}{\partial r} = \frac{\phi_{out}(R,\theta)}{R} - R\int_{\pi}^{\theta}\sigma_{r\theta}(R,\theta)d\theta \qquad (10)\\
&\frac{\partial^2\phi_{out}(R,\theta)}{\partial r^2} = \sigma_{\theta\theta}(R,\theta)
\end{aligned}$$

where $f(R,\theta) = \sigma_{rr}(R,\theta) + \int_{\pi}^{\theta}\sigma_{r\theta}(R,\theta)d\theta$.

The integration can be carried out by using a numerical method. Knowing the stress distribution at the circle boundary $r=R$, the stress function and its derivatives of the outer field with respect to r can be obtained from (10).

By using the energy variational method and the boundary conditions (10), we carry out detailed computations of the stress fields for a single edge cracked panel (SECP) with three a/w ratios, a/w = 0.1,0.5, and 0.9, where a is the crack length and w the specimen width. When the crack is short, the uncracked ligament is essentially subjected to tension; while the uncracked ligament is essentially subjected to bending when the crack becomes longer,. So the triaxiality near the crack tip varies with the crack length. Different loading levels are chosen such that the plastic deformations develop from small-scale yielding to full yielding. The values of the material properties used in the calculations are n=10, E/σ_0 = 300, ν=0.3 and α=1. A general-purpose finite-element program developed by le Centre d'Energie Atomique de France, named CASTEM 2000, is used for preliminary computations.

The outer field, represented by the stress distribution at the circle boundary $r=R$, is evaluated by the finite element method. These stress components are converted into the stress function and its derivatives by using (10). The choice of the radius R does not influence much the accuracy of the calculation. However, this radius cannot be too long because the inner field is approached only by a four-term expansion. In this work, $R=0.05w$ is chosen for specimens with short cracks, while $R=0.09w$ is chosen for specimens for long cracks.

The near-tip asymptotic field, described by the first term of expansion (3), is characterized by the J-integral which can be determined in the finite element modelling. The virtual crack extension method developed by PARKS [4], implemented in the CASTEM 2000 program, is used to calculate the J-integral. Knowing the value of the J-integral , the amplitude of the HRR solution can be determined.

Then the first term of the inner field and the outer field are approached by polynomial functions as described in (4) and (5). Thus all the coefficients in the stress function of the inner field can be obtained by a simple matrix multiplication (6).

The different exponents s_1, s_2, s_3 can be calculated by minimizing the complementary energy in the structure. The numerical procedure used in this work is the downhill simplex method. This method is easy to use to find out the minimum of a function with more than one independent variable. With this method, the exponent vector { s_1, s_2, s_3} can be found. The convergence is guaranteed by this method for any initial simplex

guessed . However, a local minimum point may be reached. So it is preferable to proceed to several downhills with different initial simplexes. The optimal point can be chosen after survey of the results.

Results and Discussions

Complete stress fields around the crack tip

The power exponents in expansion (3) obtained for SECP's with different crack lengths and loading levels are listed in Table 1. Table 1 shows that in all cases studied in this work, a 4-term expansion (including the HRR solution) is sufficient to connect accurately the inner elastic-plastic stress field near the crack tip to the far outer field. The exponent of the last term is often very big. This means that its influence on the near tip stress distribution is very small, nearly negligible. It is also seen that the inner field extends largely over distances of $5J/\sigma_0$ encompassing length scales in the cleavage fracture process zone, both in small- and large-scale yieldings.

Table 1: Power exponents in the expansions of the complete solution

a/w	*R/w*	*J*	yielding	s_0	s_1	s_2	s_3
			(N/mm) scale				
0.1	0.05	2.77	SSY	1.909	2.65	2.74	30
0.1	0.05	15.99	MSY	1.909	2.03	2.96	85
0.1	0.05	63.93	LSY	1.909	2	2.85	200
0.5	0.05	3.17	SSY	1.909	2.58	2.69	9.46
0.5	0.05	13.82	MSY	1.909	2.30	2.48	250
0.5	0.05	72.29	FY	1.909	2.15	5.35	128
0.9	0.09	2.77	SSY	1.909	2.65	2.74	28
0.9	0.09	15.99	MSY	1.909	3.60	3.65	3.70
0.9	0.09	30.16	FY	1.909	3.42	3.45	3.51

In order to verify the results of this approach, we compare the complete solutions with those of the finite element method. The results of such comparisons are presented in Fig. 1.

The angular distributions of the stress components are illustrated for distances $r \cong 2J/\sigma_0$ from the crack tip, while the radial distributions are presented along the uncracked ligament near the crack tip within distances $r < 10J/\sigma_0$. Fig. 1 shows a total agreement between the complete solutions of the energy method and those of the finite element method for short and long cracks under SSY and LSY conditions. This means that a four-term expansion can accurately describe the inner stress field near the crack tip which is connected to the far field of any real engineering structure. These results confirm those obtained by LI [3] for whom the first term in pure elastic expansion was used as the far outer field.

It must be noted that the complete solution obtained in this work by using the small deformation theory are accurate only beyond certain distances from the crack-tip, of the order of $2J/\sigma_0$ (MCMEEKING, [5]). Within these distances, the results may be erroneous compared with those obtained with the limit deformation theory. But in general, the zone within $r = 2J/\sigma_0$ is small compared with the plasticity extent. Therefore, the complete solution is accurate enough to represent the stress distribution near the crack-tip.

In recent studies, the criterion proposed by RITCHIE *et al.* [6], known as RKR criterion, was often used to predict the cleavage propagation of an elastic-plastic crack. According to this criterion, the cleavage fracture requires achieving a critical normal stress σ_c at a critical distance r_{ic} along a line where the normal tensile stresses are maximum. This line, if called cleavage line, must be one of the trajectory lines of the principal stresses starting from the crack tip. In the mode I problem, the cleavage line is just along the uncracked ligament ahead of the crack tip. However, in the mixed mode problem, this line may not be a straight line ahead of the crack tip. In this case, the cleavage line can be obtained only if the complete solution is known. In this work, the possibility to obtain the cleavage line in the mode I problem is presented. The cases for the mixed mode will be the subject of forthcoming studies.

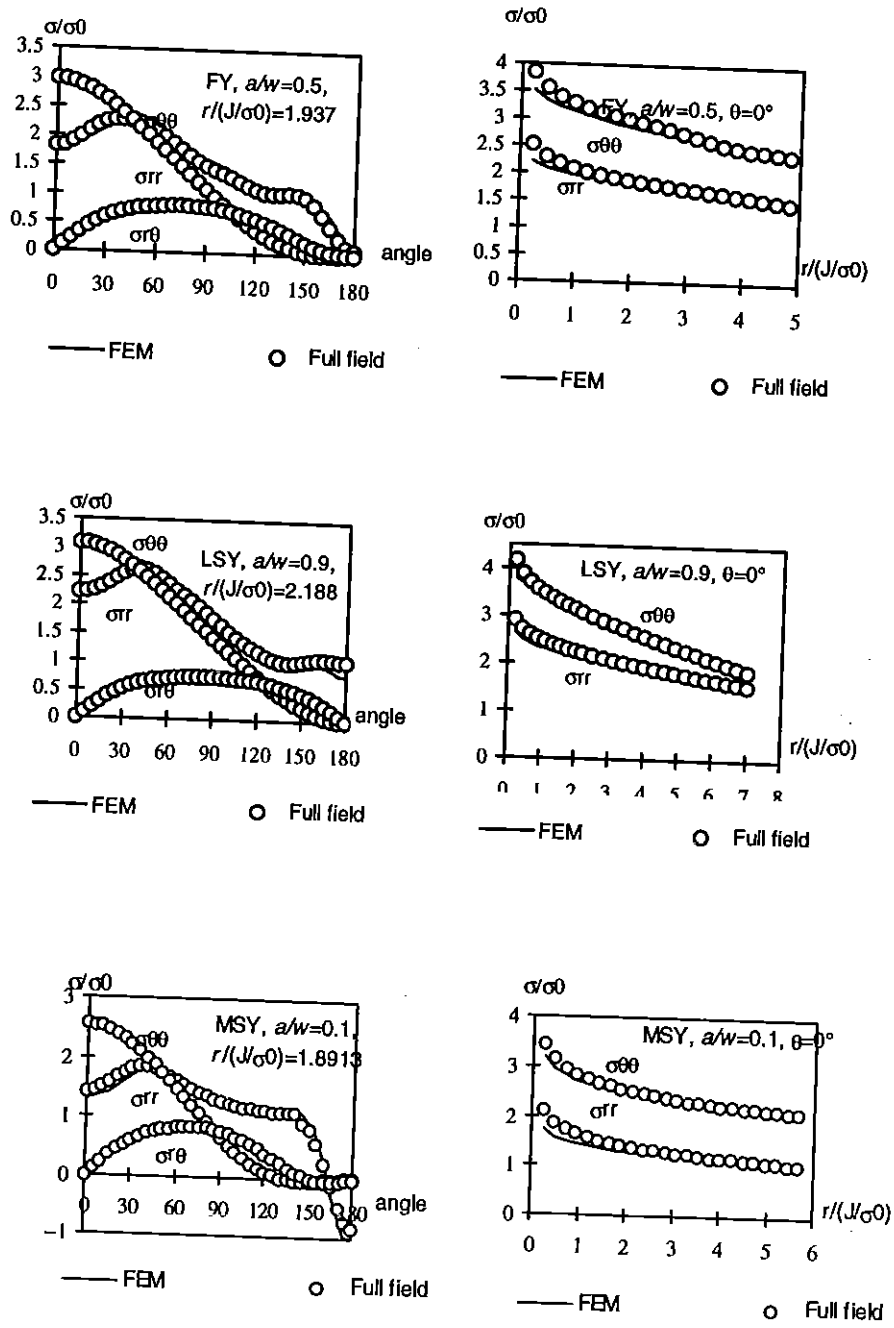

Fig.1: Comparison of the stress fields between the results of the finite element modelling and of the complete solution

Cleavage fractures

The trajectory lines of the principal stresses for the in-plane problem are easy to obtain by using the Mohr circle technique if the stress field is known. By using the complete solution mentioned above, the trajectory lines of the principal stresses of SECP specimens are drawn both for a short crack (a/w=0.1) and a long crack (a/w=0.9) as shown in Figure 2. From Fig. 2, one can see that the principal stresses near the crack tip always follow the direction of the crack plane by forming a "cleavage band". This means that if the crack grows in the cleavage mode, it will always follow this cleavage band. The heterogeneity of the material may perturb the growth direction on microstructural scale. However, the crack growth on macroscopic scale must be governed by the cleavage band. Fig. 2 also shows that the trajectory field of the principal stresses of a short-cracked specimen are quite different from that of a long-cracked one. In a short-cracked specimen, where the uncracked ligament is essentially subjected to tension, the cleavage band stretches quite far away from the crack tip; while in a long- cracked specimen, where the uncracked ligament is essentially subjected to bending, the cleavage band stops at a neutral point beyond which the ligament is subjected to compression.

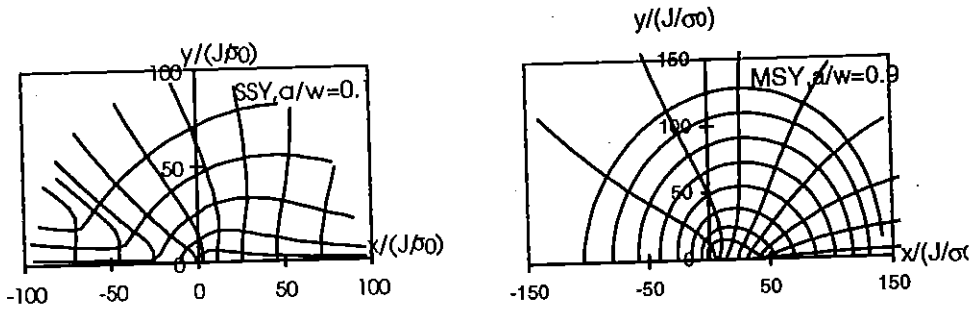

Fig.2: Trajectory line fields of the principal stresses near the crack tip for a/w=0.1 and 0.9.

It is necessary to note that the finite element solution can also provide such trajectory fields by using a special post-procedure. However, the complete solution makes this work easier and more accurate.

Slip fractures

If the crack propagates in a ductile manner, the plasticity will progress from the crack tip until a characteristic size is reached along a maximum shear stress direction, before a fracture is observed. Few criterion studies have dealt with this type of fractures so far. However, slip fractures have been observed in many experimental studies. SHIH and GERMAN [7] reported that they occurred in A533B steel center-cracked panels (CCP) under tensile loads when the cracks were deep enough. They also noted that the slip fracture toughness was almost twice as high as that of the cleavage fractures.

Slip fractures can be studied if one knows the complete solution of the stress field around the crack tip. In an elastic-plastic bidimensional structure, the plasticity progresses along the planes of the maximum shear stresses. The maximum shear stress at a point can be calculated when the three principal stresses are known:

$$\tau_{max} = (\sigma_1 - \sigma_3)/2 \qquad (11)$$

where σ_1 is the maximum principal stress and σ_3 is the minimum principal stress. The direction of τ_{max} is at 45° with respect to σ_1 and σ_3. In the case of plane strain under tensile loads, the maximum principal stress σ_1 is always in the structure plane, i.e. in the XY-plane. However, the minimum principal stress σ_3 may be in the XY-plane or in the direction perpendicular to it, i.e. along the Z-axis. Whether σ_3 is in the XY-plane or along the Z-axis, the region near the crack tip can be divided into several different zones. In the zones belonging to the first case, say zones I, the maximum shear stress τ_{max} is in the XY-plane too. In the zones belonging to the second case, say zones II, τ_{max} is at 45° with respect to the XY-plane. Fig. 3 shows the division of the region near the crack tip into such zones for SECP's according to our calculations. For shorter cracks, zone II is an open area and limited by $|\theta|<30°$. For longer cracks, this zone is a closed area and bounded by $|\theta|<40°$ near the crack tip.

The division of the region into such zones is important insofar as the plasticity developments are different in the two zones. If the plasticity progresses in zones I, one part of the structure will slip with respect to another part along the direction of τ_{max} in the

XY-plane. However, if the plasticity develops in zone II, the global slipping at 45° to the XY-plane cannot be observed due to the thickness of the structure. Slipping on a microstructural scale is transformed into an axial deformation in the XY-plane.

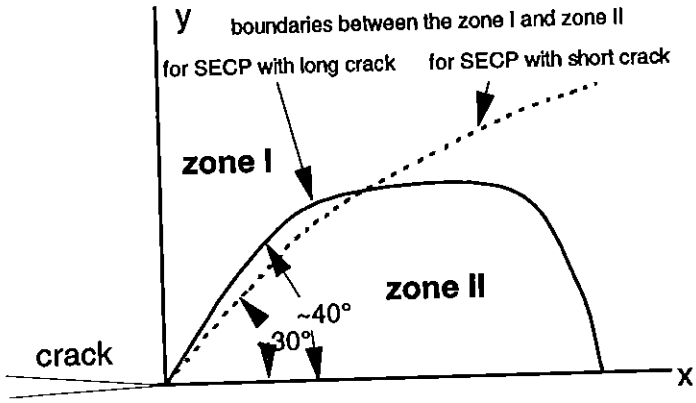

Fig.3: Division of the region near the crack tip into zone I and zone II

Since the maximum shear stresses in zones I are situated in the XY-plane, the growth direction of a ductile crack can be determined by drawing the trajectory lines of the maximum shear stresses near the crack tip. The complete solutions facilitate this work. Fig. 4 shows these trajectory line fields of SECP's for different crack lengths and loading levels. Observation of Fig. 4 shows that the trajectory lines of the maximum shear stresses concentrate in several directions from the crack tip by forming some "slip bands". One can observe 3 slip bands for all specimen geometries considered: the first with $\theta \cong 50°$, the second with $\theta \cong 100°$ and the third with $\theta \cong 140°$. From Fig. 4, it is observed that all these slip bands are situated in zone I. One can also note that from any point situated in the vicinity of the crack tip, the trajectory lines of the maximum shear stresses will follow one of the three slip bands. This means that if the plasticity develops in the vicinity of the crack tip, it will progress in one of these directions and will cause the structure to slip in the XY-plane.

From Fig.4, one can clearly observe the difference between the direction of the first slip band of a short-cracked SECP and that of a deeply-cracked one. The first slip band in the short-cracked SECP is oriented at about 45° with respect to the crack plan. The orientation angle is bigger when the crack becomes longer. It can reach 65° for a deeply-cracked SECP. This phenomena shows that the slip mode for a crack essentially subjected

to tension is quite different from that for a crack essentially subjected to bending.

Calculation shows that the maximum shear stresses along the third slip band are smaller than those along the first two. Therefore one can conclude that the crack has little probability to grow in this direction. However, the magnitude of the maximum shear stresses along the first slip band is comparable to that along the second. Fig.5 shows the maximum shear stresses along these two slip bands in a short cracked specimen and in a long-cracked one. From Fig. 5, one can observe that the maximum shear stresses along the second slip band are higher than those along the first within a certain distance from the crack tip, and then become lower beyond this distance. The high shear stresses along the second slip band near the crack tip may cause the crack opening which can be observed in plastic material. However, the maximum shear stresses rapidly decrease along the second slip band. The plasticity is constrained by the geometry of the specimen. It does not develop sufficiently, so that the crack cannot initiate in the ductile manner along this direction. This may explain why few slip fractures in this direction have been observed in experimental studies. On the other hand, the maximum stresses along the first slip band are higher than those along the second for long distances. Therefore, the plasticity will develop essentially along this direction. One can conclude that the slip fracture will essentially occur along the first slip band under mode I loading.

It is also important to note that the maximum shear stresses along the two slip bands in short-cracked SECP's are higher than those in deeply-cracked SECP's. This explains why the slip fractures are often found in specimens whose uncracked ligaments are essentially subjected to tension.

These remarks do agree with the experimental results. The experimental studies of SHIH and GERMAN [7] about the deeply-cracked CCP's of A533B steels showed that slip fracture occurred in the direction of about 45° to the crack plane. The analysis of the slip bands of the full stress field in this work predicts exactly the same direction for low-hardening plastic materials.

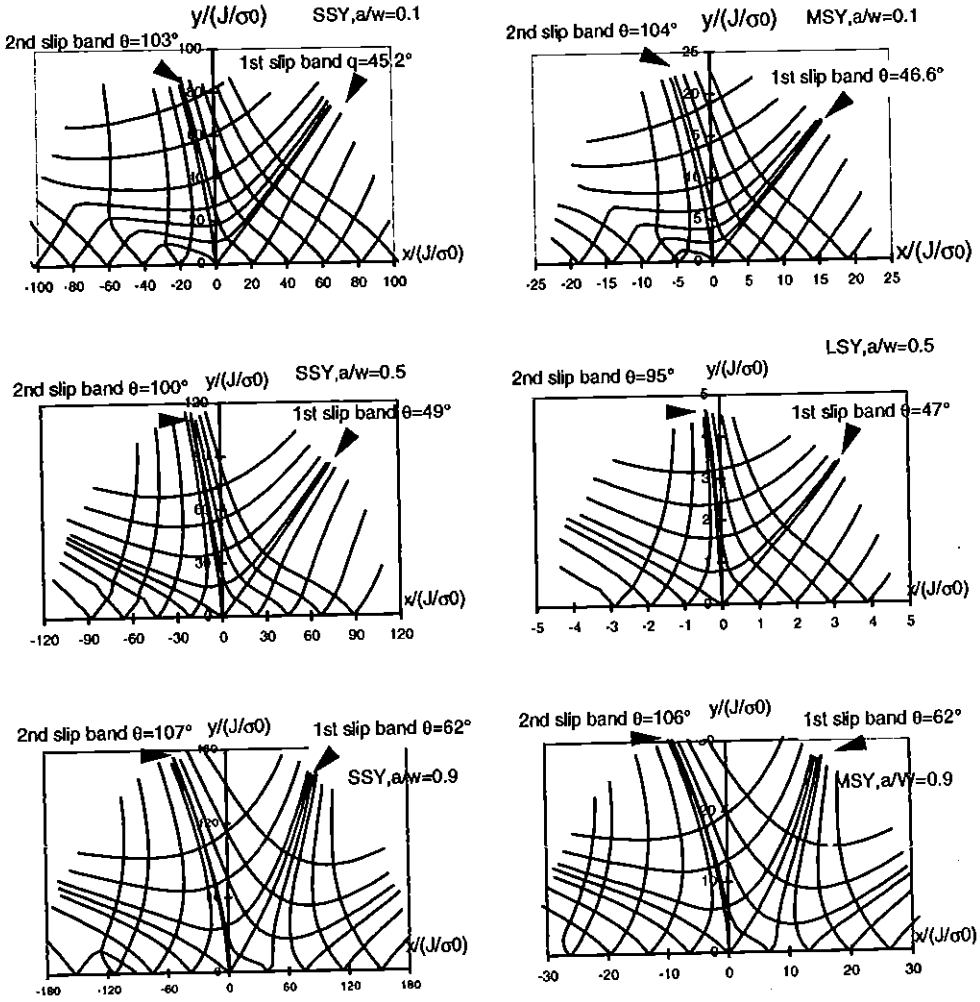

Fig.4: Trajectory line fields of the maximum shear stresses

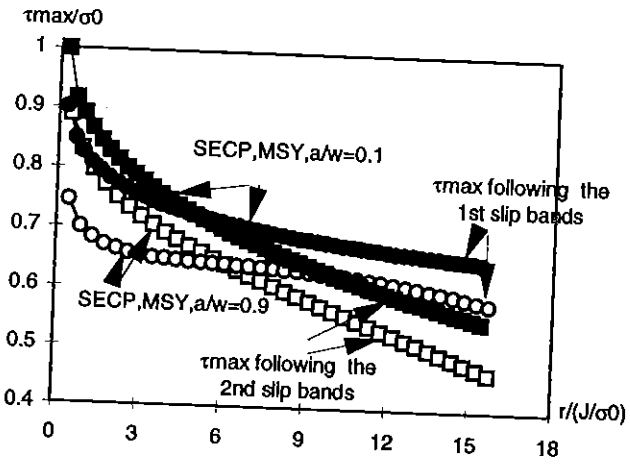

Fig.5: Maximum shear stresses along the first two slip bands for a/w=0.1 and 0.9.

Competition between cleavage and slip fractures

The analysis of the trajectory line fields of the principal stresses and of the maximum shear stresses enables us to determine the cleavage bands and the slip bands of cracked structures. However, such an analysis cannot predict in which direction the crack will grow. To answer this question, these two modes of fractures must be put into competition.

We first suppose that the RKR criterion can be extended to the slip fracture: the crack will grow along one of the slip bands if a critical shear stress τ_c at a critical distance r_{IIc} along this slip band is reached. τ_c and r_{IIc} are material constants and their values can be determined experimentally. They are supposed to be independent from the slip band orientation. According to the remarks in the above section, we can suppose that, in most cases, the slip fracture occurs only along the first slip band ($\theta \cong 45\sim60°$).

These hypotheses lead to the following criteria:

Let $\sigma(r_{Ic})$ be the maximum principal stress at a characteristic distance r_{Ic} along the cleavage band and $\tau(r_{IIc})$ the maximal shear stress at a characteristic distance r_{IIc} along the slip band. The crack will grow along the cleavage band if

$$\sigma(r_{Ic}) > \sigma_c \quad \text{and} \quad \frac{\sigma(r_{Ic})}{\tau(r_{IIc})} > \frac{\sigma_c}{\tau_c} \tag{12}$$

The crack will grow along the slip band if

$$\tau(r_{IIc}) > \tau_c \quad \text{and} \quad \frac{\sigma(r_{Ic})}{\tau(r_{IIc})} < \frac{\sigma_c}{\tau_c} \tag{13}$$

It is necessary to note that r_{IIc}, as opposed to r_{Ic} which is often considered as a microstructural quantity, must be a macroscopic quantity, since the plasticity near the crack tip in a ductile material generally extends over a rather large area, comparable to the size of the crack length .

In fact, criteria (12) and (13) describe the competition between cleavage and slip fractures, or between mode I and mode II fractures of a ductile crack. These criteria can also be applied to the mixed mode problem if the stress field near the crack tip is known. It is clear that these criteria may also include the critical strain values. MCMEEKING [5] considered that the cleavage fracture might suggest a stress-controlled process while the slip fracture seemed to suggest a plastic strain-dominated process. From this point of view, mixed criteria may be more adequate to involve predictions of the transition of the fracture mode. The choice of the critical quantities will depend on the results of experimental studies.

In order to show the trend of the crack growth, we simulate such a competition for SECPs under different loading levels. We suppose artificially r_{Ic}=0.05 and r_{IIc}=0.5 in this simulation. The characteristic stresses $\sigma(r_{Ic})$ and $\tau(r_{IIc})$ are calculated for different crack lengths and represented against the value of the J-integral as shown in Figure 6.

From Fig. 6, it is observed that when the loading level is low, the values of $\sigma(r_{Ic})$ are nearly identical for all initial crack lengths. As the loading level increases, the values of $\sigma(r_{Ic})$ increase at different rates for differently-cracked specimens. In the specimen with a/w=0.9, $\sigma(r_{Ic})$ increases more rapidly than in the other two specimens (a/w=0.5 and 0.1). It is when a/w=0.1 that $\sigma(r_{Ic})$ increases the most slowly. This means that the triaxial tension level in the vicinity of the crack tip increases more rapidly in bending-loaded specimens than in tension-loaded ones as the remote loads increase. The opposite phenomenon is observed for the values of $\tau(r_{IIc})$. In this case, the maximum shear stress $\tau(r_{IIc})$ is higher in the short-

cracked SECP (a/w=0.1) than in the deeply-cracked ones (a/w=0.5 and 0.9). Therefore one can conclude that in bending-loaded specimens, the cleavage fractures are more probable. On the other hand, in tension-loaded specimens, the slip fractures are more probable. They will occur if condition (13) is reached.

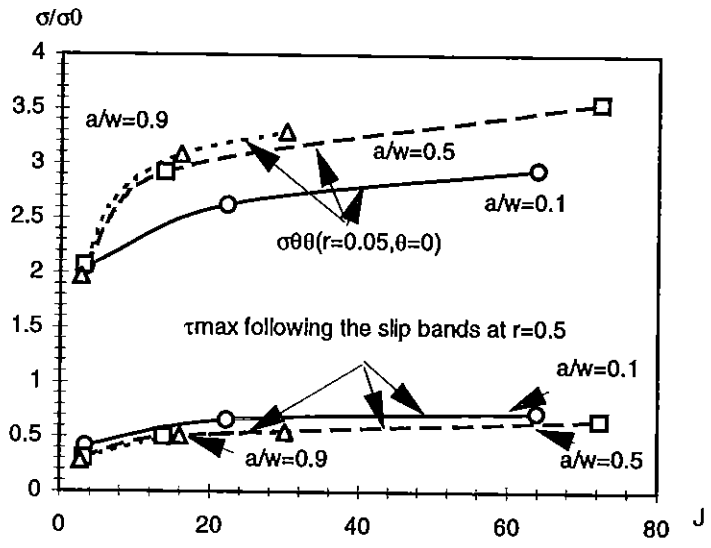

Fig.6: Competition between the characteristic stresses $\sigma(r_{Ic})$ and $\tau(r_{IIc})$ in SECP specimens.

Conclusions

An energy variational method has been proposed to study the complete solution of the stress field near a stationary, plane strain, mode I crack in a power-law hardening material. In association with the finite element method, this analysis can be used in real engineering structures. It is shown that in general, a four-term expansion of the stress function is sufficient to describe the stress field accurately, near or far from the crack tip. This property allows us to examine the plasticity progression which can extend over a large region before a slip fracture occurs.

By using the Mohr circle technique, the trajectory fields of the principal stresses and the maximum shear stresses have been drawn from the complete solution in order to determine the crack growth direction. One notices that the crack can progress along a "cleavage band" or along a "slip band" according to the triaxial tensile stress level in the vicinity of the crack. These bands can easily be found from the trajectory fields. The growth direction of a ductile crack finally depends on the competition of the stress concentrations along these bands. Based on the RKR model, criteria (12) and (13) have been proposed to judge such a competition. According to these criteria, cracks in bending-loaded specimens show higher probability to grow along the crack plane since condition (12) dominates the competition, while cracks in tension-loaded specimens may initiate at a certain angle to the crack plane if (13) is satisfied. It must be noted that the criteria proposed in this study will have to be confirmed in further definitive experiments giving σ_c (or J_c),and τ_c values.

References

[1] Hutchinson J.W., (1968) *J. Mech. Phys. Solids* **16**, 13-31

[2] RICE J.R.and ROSENGREN G.F. (1968) *J. Mech. Phys. Solids* **16**, 1-12

[3] LI J.(1997) *Int. J. Fracture*, (to appear in 1997).

[4] PARKS D.M. (1974) *Int. J. Fracture* **10**, 487-501

[5] MCMEEKING R.M. (1977) *J. Mech. Phys. Solids* **25**, 357-381

[6] SHIH C.F.and GERMAN M.D. (1981) *Int. J. Fracture* **17**,27-43

[7] RITCHIE R.O, KNOTT J.F. and RICE J.R. (1973) *J. Mech. Phys. Solids* **21**, 395